IEEE Photonics Journal
An IEEE Photonics Society Publication

Open Access

Simultaneous Measurement of MDL and DMGD in FMFs by Analyzing the Rayleigh Backscattering Amplitudes

Volume 11, Number 2, April 2019

Feng Liu
Guijun Hu
Weicheng Chen
Cuiguang Chen
Congcong Song
Jiake Chen

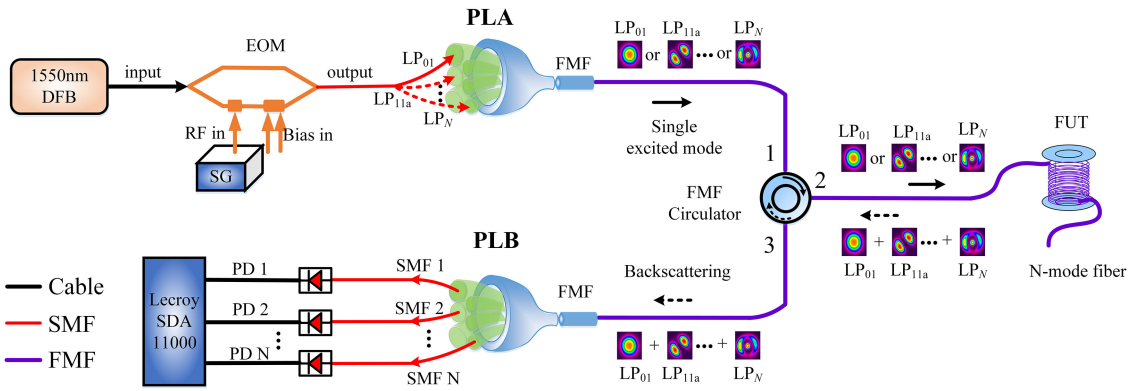

DOI: 10.1109/JPHOT.2019.2901263
1943-0655

Simultaneous Measurement of MDL and DMGD in FMFs by Analyzing the Rayleigh Backscattering Amplitudes

Feng Liu, Guijun Hu, Weicheng Chen, Cuiguang Chen, Congcong Song, and Jiake Chen

College of Communication Engineering, Jilin University, Changchun 130012, China

DOI:10.1109/JPHOT.2019.2901263

Manuscript received September 4, 2018; accepted February 19, 2019. Date of publication February 25, 2019; date of current version March 12, 2019. This work was supported in part by the grant from the National Natural Science Foundation of China (NSFC) (No. 61575078), and in part by Jilin Provincial Science and Technology Department (No.20190302014GX). Corresponding author: Guijun Hu (e-mail: hugj@jlu.edu.cn).

Abstract: In this paper, we propose and experimentally demonstrate a novel method for simultaneously measuring mode-dependent loss (MDL) and differential modal group delay (DMGD) in few mode fibers (FMFs). This method is based on analyzing the Rayleigh backscattering amplitudes obtained with a special nondestructive measurement system. With this method, the MDL and DMGD in about 9.8 km 3-mode fiber are successfully measured, which are 0.186 dB and 3.581 ps/m between LP_{01} and LP_{11a} and 0.157 dB and 3.604 ps/m between LP_{01} and LP_{11b}, respectively. Then, the experimental results of DMGD and MDL with different methods are compared, which show that the values of DMGD and MDL obtained by the proposed method agree well with that using the time-of-flight (TOF) and conventional transmission methods, respectively. In addition, it is also demonstrated that the proposed scheme can be scalable to measure FMFs with a large number of modes.

Index Terms: Few mode fiber, Rayleigh backscattering, mode dependent loss, differential modal group delay.

1. Introduction

As a promising solution to the forthcoming capacity crunch of long-haul single-mode fiber (SMF) systems, mode-division multiplexing (MDM) transmission system using few-mode fibers (FMFs) has recently been intensively studied [1]–[4]. The MDM technology utilizes the orthogonal spatial mode of FMF as the new multiplexing dimension to carry information independently. Ideally, the capacity of a MDM system is proportional to the number of modes. However, the practical FMF-based MDM systems need to take some additional FMF impairments into consideration, which mainly include mode-dependent loss (MDL), differential modal group delay (DMGD) and mode coupling (MC), etc. MDL and DMGD, which respectively characterize the different transmission losses and group velocities between modes, are the most critical issues in relation to FMF-based MDM systems. When a large MDL and DMGD are accumulated in FMF transmission links, the computational complexity of multiple-input-multiple-output (MIMO) equalization can be unmanageable for MDM system, which deteriorate the transmission performance and limit the transmission distances of MDM systems [5]–[8]. In order to optimize the performance of MDM systems and optimize

the FMF designing scheme, characterizing FMFs accurately is of great significance. Efficient techniques that can measure MDL and DMGD conveniently and precisely become an imperative requirement.

Several techniques for measuring the DMGD in FMF have been proposed, such as optical low-coherence interferometry (OLCI) technique [9], time-of-flight (TOF) method [10] and spectral interferometric technique [11]. However, the complicated experimental setups or expensive equipment are required for both the TOF and OLCI, and thus may not be easily accessible. The spectral interferometric method has a limit to the length of reference arm, which is difficult to measure the impairment parameter of a long FMF. Recently, the microwave-photonic, electrical spectral interferometry, and coherent-detection-based method with some sophisticated algorithms techniques [12]–[15] have been demonstrated for characterizing FMFs with good accuracy, which might not be cost-effective. In terms of MDL measurement, it is essential to separate the propagating modes. The MDL is always measured with cutback or insertion methods combining mode multiplexers or mode converters, such as mode couplers or phase plates [16]. But these methods are destructive. Therefore, some new techniques should be researched to characterize the property of a long FMF installed in the large-capacity MDM transmission systems. Recently, nondestructive technique for measuring the mode coupling (MC) in the FMFs and multi-core fibers (MCFs) has been proposed using synchronous multi-channel optical time domain reflectometry (OTDR) [17], [18]. Meanwhile, the bidirectional OTDR technique has been adapted for FMFs or MCFs to measure mode field diameter (MFD) distribution, relative-index difference, chromatic dispersion (CD) and so on [19]–[21]. However, there have been few reports on OTDR technique for measuring the MDL or DMGD in FMFs, especially for simultaneous measurement of above two impairments.

In this paper, we propose and experimentally demonstrate method for simultaneously measuring the MDL and DMGD in the FMFs. The MDL and DMGD can be simultaneously measured with the proposed method based on analyzing the Rayleigh backscattering amplitudes obtained using a nondestructive measurement system. The measured MDL and DMGD in 3-mode fiber are about 0.186 dB and 3.581 ps/m between LP_{01} and LP_{11a}, 0.157 dB and 3.604 ps/m between LP_{01} and $LP_{11b,}$ respectively. The experimental results show that the values obtained with the proposed method agreed well with that obtained with the conventional transmission and TOF methods, respectively. Moreover, the proposed scheme is scalable to measuring fibers with a large number of modes.

The rest of the paper is organized as follows: Section 2 discusses the principle for simultaneous measurement of MDL and DMGD in FMF. In Section 3, the measurement performance of our proposed method is verified by experiment, and then we compared the proposed method with the TOF and conventional transmission methods, respectively. Section 4 demonstrates the ability of proposed method for measuring fibers with large number of modes. Finally, conclusions are drawn in Section 5.

2. Principle for Simultaneous Measurement of MDL and DMGD

We utilize the Rayleigh backscattering amplitudes obtained with an optical reflectometry technique to simultaneously measure the MDL and DMGD in FMFs. In order to derive the equation for mode-resolved time-dependent amplitudes of Rayleigh backscattering at the front end of the FMF, we assumed that an optical pulse with a temporal width of ΔT and a peak power P_0 is launched at $z = 0$ into mode LP_i. The time-dependent amplitude of Rayleigh backscattering in mode LP_j received at $z = 0$ can be calculated by Eq. (1) [22], [23]. We use subscripts i and j ($i, j = 1, 2, 3, \ldots, N$) to represent the mode labels (01, 11a, 11b...) of FMF, respectively.

$$P_{i,j}^{BS}(t) = P_0 \alpha_s B_{i,j} \bar{\nu} \Delta T e^{-2\bar{\alpha}\bar{\nu}t} \tag{1}$$

where $\bar{\nu} = \frac{\nu_{gi}\nu_{gj}}{\nu_{gi}+\nu_{gj}}$; $\bar{\alpha} = \frac{\alpha_i+\alpha_j}{2}$; ν_{gi} and ν_{gj} are the attenuation coefficients of modes LP_i and LP_j, respectively; α_i and α_j are the attenuation coefficients of modes LP_i and LP_j, respectively; $B_{i,j}$ is the overall backscattering capture coefficient, which is quantifies the ratio of the energy coupled

into back-propagating mode LP_j over the total energy of Rayleigh backscattering excited by forward transmission mode LP_i; α_s is the Rayleigh scattering coefficient, which is defined as the ratio of total backscattered energy to incident energy. Thus, Eq. (1) can be approximated as

$$P_{i,j}^{BS}(t) = P_0 \alpha_s B_{i,j} \frac{v_{gi} v_{gj}}{v_{gi} + v_{gj}} \Delta T \exp\left[-(\alpha_i + \alpha_j) \frac{v_{gi} v_{gj}}{v_{gi} + v_{gj}} t \right] \tag{2}$$

According to Eq. (2), the backscattered amplitude of mode LP_j with time-varying can be derived as:

$$P_{i,j}^{BS}(t)(dB) = -\left[(\beta_i + \beta_j) \frac{v_{gi} v_{gj}}{v_{gi} + v_{gj}} \right] t + \left[10\log_{10}\left(P_0 \alpha_s B_{i,j} \frac{v_{gi} v_{gj}}{v_{gi} + v_{gj}} \Delta T \right) \right](dB) \tag{3}$$

where $\beta_i = 4.343\alpha_i$ and $\beta_j = 4.343\alpha_j$. In order to facilitate the analysis, the Eq. (3) can be simplified to $P_{i,j}^{BS}(t)(dB) = -\psi_{i,j} t + \gamma_{i,j}(dB)$, and the $\psi_{i,j}$ and $\gamma_{i,j}$ represent the slope and intercept of the linear regression (LR) line for the Rayleigh backscattering amplitudes, respectively. According to Eq. (3), when an input optical pulse is coupled into the mode LP_i of FMF, the backscattered amplitude of mode LP_i can be written as follows:

$$P_{i,i}^{BS}(t)(dB) = -(\beta_i v_{gi}) t + \left[10\log_{10}\left(P_0 \alpha_s B_{i,i} \frac{v_{gi}}{2} \Delta T \right) \right](dB) \tag{4}$$

Similarly, when optical pulse is coupled into the mode LP_j $(i \neq j)$, the backscattered amplitude of mode LP_j is given as

$$P_{j,j}^{BS}(t)(dB) = -(\beta_j v_{gj}) t + \left[10\log_{10}\left(P_0 \alpha_s B_{j,j} \frac{v_{gj}}{2} \Delta T \right) \right](dB) \tag{5}$$

According to the slops $\psi_{i,j}$, $\psi_{i,i}$, $\psi_{j,j}$ and intercept $\gamma_{i,i}$ in the Eqs. (3), (4) and (5), we can thus derive the following equations:

$$\begin{bmatrix} \psi_{i,i} \\ \psi_{j,j} \end{bmatrix} = \begin{bmatrix} \beta_i v_{gi} \\ \beta_j v_{gj} \end{bmatrix} \tag{6}$$

$$\frac{v_{gi} v_{gj} (\beta_i + \beta_j)}{v_{gi} + v_{gj}} = \psi_{ij} \tag{7}$$

$$v_{gi} = \frac{2}{P_0 \alpha_s B_{i,i} \Delta T} 10^{\frac{1}{10}\gamma_{i,i}} \tag{8}$$

According to Eq. (8), the two additional parameters α_s and $B_{i,j}$ need to be measured, which cause larger measurement error. Therefore, we represent the semi-log signals for the LP_i mode measured from one end of the FUT as $S_{i,i}(t)$, and measured from the other end as $S'_{i,i}(t)$. Then, the imperfection contribution for the LP_i mode, $I_{i,i}$, can be written as follows:

$$I_{i,i} = \frac{S_{i,i}(t) + S'_{i,i}(\tau - t)}{2} = 10\log_{10}(\alpha_s B_{i,i}) + 10\log_{10}\left(P_0 \frac{v_{gi} \Delta T}{2} \right) - 5\log_{10}\left[\exp(2\alpha_i v_{gi} \tau) \right] \tag{9}$$

where $\tau = \frac{L}{v_{gi}}$, and L is length of the FUT. Then, with Eqs. (8) and (9), we can obtain the Eq. (10). This method does not need to measure the above two parameters separately, so as to effectively improve the measurement accuracy.

$$\beta_i = \frac{1}{L}(\gamma_{i,i} - I_{i,i}) \tag{10}$$

Then, these unknown coefficients v_{gi}, v_{gj}, β_i and β_j are solved with Eqs. (6), (7) and (10). Moreover, four unknown parameters can also be calculated without the information of $\psi_{i,j}$ by measuring $I_{j,j}$ and $\gamma_{j,j}$ additionally. In this paper, because we mainly measure the MDL and DMGD between fundamental mode (LP_{01}) and higher order modes. Therefore, in order to reduce double-end measurement times and the number of measurement parameters, we took LP_{01} mode as the benchmark, i.e., we calculated the parameters of β_i, β_j, v_{gi} and v_{gj} by measuring $\psi_{i,j}$, $\psi_{i,i}$, $\psi_{j,j}$, $\gamma_{i,i}$ and $I_{i,i}$. Thus, the $DMGD_{i,j}$ and $MDL_{i,j}$ between mode LP_i and mode LP_j can be simultaneously calculated by substituting the

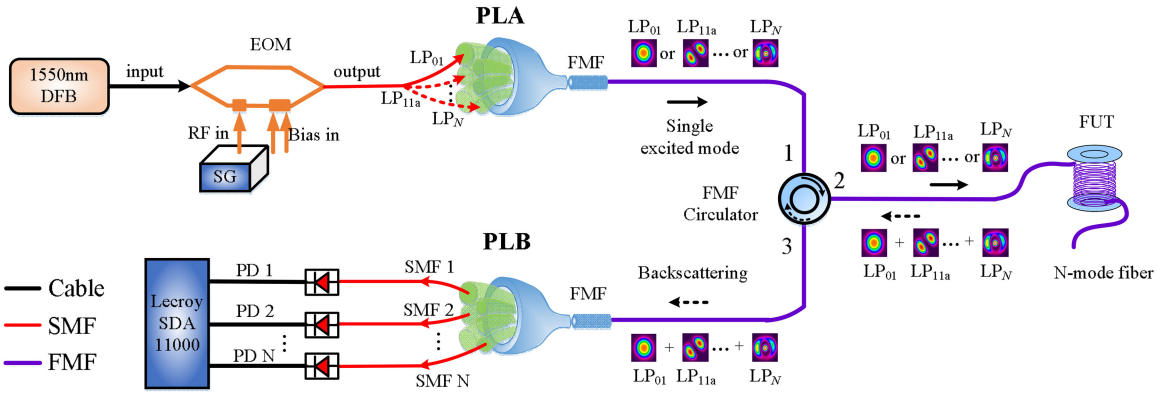

Fig. 1. Experimental setup for simultaneously measuring MDL and DMGD in FMFs. DFB: continuous wave source; EOM: Electro-optic modulator; SG: signal generator; PL: Photonic Lantern; PD: photodetector; FUT: fiber under test.

parameters calculated above into the equations $DMGD_{i,j} = |1/v_{gi} - 1/v_{gj}|$ and $MDL_{i,j} = |\beta_i - \beta_j|L$, respectively.

3. Experimental Setup and Results

The proposed measurement setup for simultaneously measuring MDL and DMGD is shown in Fig. 1. We use a distributed feedback laser (DFB) as the light source. The DFB generates a continuous-wave light, which is modulated by an electro-optic modulator (EOM) driven by a signal generator (SG) to generate input optical pulse. The spacial mode conversion is realized by the mode converter. The optical pulse entering into the mode converter through the LP_i ($i = 1, 2, 3, \ldots, N$) port can be converted into the corresponding excited mode and emitted from the FMF pigtail of the mode converter. Then, the optical pulse is coupled into the fiber under test (FUT) through the FMF circulator and the backscattered light is generated through the entire transmission, which includes both the excited mode LP_i and unexcited modes LP_j ($j = 1, 2, 3, \ldots, N$). When the mixed-mode backscattered lights are returned into the mode demultiplexer through the FMF circulator, they are demultiplexd into the individual modes. The backscattered light in each channel is converted into the electrical signal by photodetectors (PDs), and then sampled by time-domain sampling scope (TDS). After the measured signals are averaged, the traces of Rayleigh backscattering amplitudes can be acquired. The amplitude data is to be processed offline using MATLAB program.

We carried out experiments to demonstrate the feasibility. We first present experimental results for a three-mode fiber that supports LP_{01}, LP_{11a} and LP_{11b} modes. The general results of (6), (7) and (10) for a FMF supporting N-modes can be specialized to the case of the 3-mode fiber. In this case, the unknown coefficients v_{g1}, v_{g2}, β_1 and β_2 for LP_{01} and LP_{11a} modes can be acquired by

$$\begin{bmatrix} \psi_{1,1} \\ \psi_{2,2} \end{bmatrix} = \begin{bmatrix} \beta_1 v_{g1} \\ \beta_2 v_{g2} \end{bmatrix} \tag{11}$$

$$(\beta_1 + \beta_2) v_{g1} v_{g2} / (v_{g1} + v_{g2}) = \psi_{1,2} \tag{12}$$

$$\beta_1 = \frac{1}{L} (\gamma_{1,1} - I_{1,1}) \tag{13}$$

Therefore, both of two impairment parameters between fundamental LP_{01} and high-order mode LP_{11a} can be simultaneously acquired by the $DMGD_{1,2} = |1/v_{g1} - 1/v_{g2}|$ and $MDL_{1,2} = |\beta_1 - \beta_2|L$. Similarly, both of them between LP_{01} and LP_{11b} can be calculated in the same way.

In our experimental setup (see Fig. 1), the mode converter and mode demultiplexer are realized using photon lantern A and B, respectively. The insertion losses (IL) of PL A and PL B used in

TABLE 1
The IL of the PL A and PL B

Insertion loss (dB)	LP_{01} port	LP_{11a} port	LP_{11b} port	LP_{21a} port	LP_{21b} port	LP_{02} port
PL A	5.467	1.549	2.194	2.932	3.411	8.984
PL B	1.167	1.278	2.094	2.802	3.365	4.390

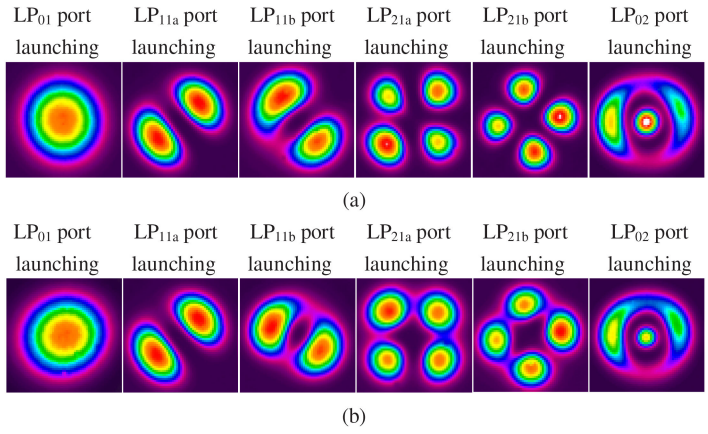

Fig. 2. Captured output mode patterns. (a) is for PL A; (b) is for PL B.

the experiment is given in the Table 1, and the captured output mode patterns are shown in the Fig. 2. Initially, a short piece of 6-FMF (2 m long) is fusion spliced to the output end of the PL A and PL B, and then the output mode patterns captured by a CCD camera are shown in Figs. 2(a) and 2(b) when we launch power from the six SMF input ports independently. As can be seen from the Fig. 2, the mode conversion and mode demultiplexing can be efficiently realized by using PL A and PL B, respectively, the mode selectivity is better. The central wavelength of DFB is 1550 nm. Each input optical pulse is a pulse width of $\Delta T = 300$ ns and peak power of $P_0 = 40$ mw. The electrical signals from the PDs are sampled by a Lecroy SDA 11000 with a sampling rate of 40 GSa/s. The measured signals are averaged 2^{16} times. The 3-mode FMF under-test, a step-index fiber, is about 9.8-km long. The port 1 of 3-mode FMF circulator is fusion-spliced with FMF-end of the PL A by core alignment, so is port 2 with the FUT and port 3 with the FMF-end of PL B.

We first carry out the measurement of $MDL_{1,2}$ and $DMGD_{1,2}$ between LP_{01} and LP_{11a} modes. Fig. 3(a) shows the Rayleigh backscattering amplitudes measured from both ends of the 3-mode fiber. The red and blue lines represent the power for the LP_{01} mode of the backscattered light measured from both ends of FUT when a 300 ns input optical pulse is coupled into the LP_{01} mode at both ends of FUT, respectively. Fig. 3(b) shows imperfection contributions for the LP_{01} mode obtained from the results of Fig. 3(a). The backscattered amplitudes of LP_{11a} mode in the FUT, when a 300 ns input optical pulse is coupled into the LP_{01} or LP_{11a} modes, are performed as shown in Figs. 4(a) and 4(b), respectively.

Note that, in order to reduce the effect of IL and crosstalk of PLs on the measurement results, we calibrated the backscattered amplitudes to compensate the IL and crosstalk occurring in spatial mode-converter (PL A) /demultiplexer (PL B) according to the following equation:

$$P_{i,j}^{BS}(t)(dB) = -\left[(\beta_i + \beta_j)\frac{v_{gi}v_{gj}}{v_{gi}+v_{gj}}\right]t + \left[10\log_{10}\left(P_0\alpha_s B_{i,j}\frac{v_{gi}v_{gj}}{v_{gi}+v_{gj}}\Delta T - \delta_{i,j}\right) - L_{i,j}\right](dB) \quad (14)$$

The $L_{i,j}$ mainly includes the IL of the spatial mode-converter (PL A) /demultiplexer (PL B) and FMF circulator. The IL of PL A and PL B used in the experiment are given in the Table 1, respectively. The IL of FMF circulator (for laser light and Rayleigh backscattering) are 0.63 dB and 0.35 dB,

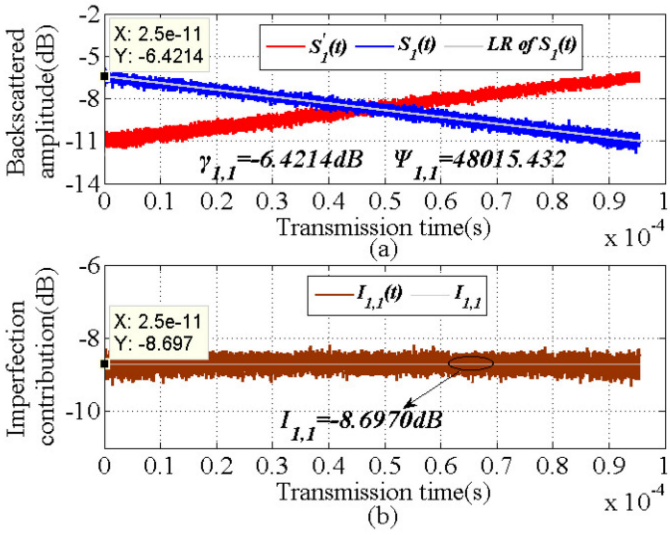

Fig. 3. The imperfection contribution $I_{1,1}$ for the LP_{01} mode. (a) Backscattered amplitudes for the LP_{01} mode measured from both ends of the FUT. (b) Imperfection contributions for the LP_{01} modes obtained from the results of Fig. 3(a).

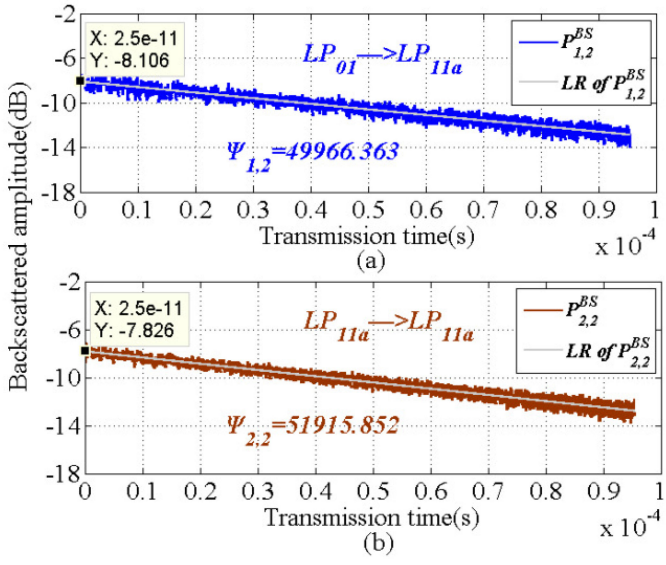

Fig. 4. Measurement results of $MDL_{1,2}$ and $DMGD_{1,2}$ between LP_{01} and LP_{11a} modes. (a) Backscattered amplitude from the LP_{11a} mode channel when a 300 ns optical pulse is coupled into the LP_{01} mode. (b) Backscattered amplitude from the LP_{11a} mode channel when a 300 ns optical pulse is coupled into the LP_{11a} mode.

respectively. In order to compensate for crosstalk caused by the PLs, firstly, the back-to-back crosstalk matrix of the PL A and PL B is measured by fusion-spliced with FMF-end of the PL A and PL B. When $i \neq j$, $\delta_{i,j} = P_0 10^{\frac{CT_{i,j}}{10}}$, the backscattered amplitudes of the unexcited mode are calibrated. When $i = j$, $\delta_{i,i} = -\sum_{j=1,i\neq j}^{N} P_0 10^{\frac{CT_{i,j}}{10}}$, the backscattered amplitude of the excitation mode is calibrated. The $CT_{i,j}$ is the crosstalk between photonic lantern mode *i* and mode *j*, as shown in Table 2.

TABLE 2
Back-to-Back Mode Crosstalk Matrix of PL A and PL B (Unit: dB)

Transfer / Receive	LP_{01}	LP_{11a}	LP_{11b}	LP_{21a}	LP_{21b}	LP_{02}
LP_{01}	---	-17.18	-16.36	-22.73	-23.81	-23.38
LP_{11a}	-19.09	---	-15.64	-16.67	-19.32	-20.74
LP_{11b}	-18.61	-14.38	---	-17.58	-18.13	-19.70
LP_{21a}	-27.67	-16.43	-16.92	---	-15.14	-19.18
LP_{21b}	-28.15	-17.62	-17.75	-14.96	---	-18.41
LP_{02}	-24.94	-19.23	-18.78	-22.34	-19.27	---

TABLE 3
The Values Of Unknown Coefficients ν_{g1}, ν_{g2}, β_1 and β_2

LP modes	ν_g [km/s]	β [dB/km]
LP_{01}	206781	0.232
LP_{11a}	206628	0.251

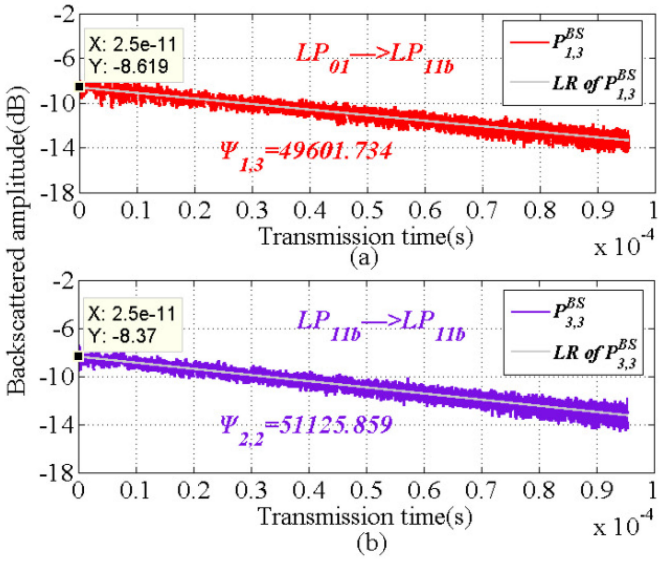

Fig. 5. Measurement results of $MDL_{1,3}$ and $DMGD_{1,3}$ between LP_{01} and LP_{11b}. (a) Backscattered amplitude from the LP_{11b} mode channel when a 300 ns optical pulse is coupled into the LP_{01} mode. (b) Backscattered amplitude from the LP_{11b} mode channel when a 300 ns optical pulse is coupled into the LP_{11b} mode.

Then, from the y axes of Fig. 3(a) at $t = 0$, $\gamma_{1,1}$ is obtained as -6.4214 dB. The imperfection contribution for the LP_{01} mode, $I_{1,1}$, can be obtain as -8.6970 dB from Fig. 3(b). The slopes $\psi_{1,1}$, $\psi_{1,2}$ and $\psi_{2,2}$ of the linear regression line are also obtained, respectively. Substituting above acquired parameters into the Eqs. (11), (12) and (13), the four unknown coefficients ν_{g1}, ν_{g2}, β_1 and β_2 can be obtained as listed in Table 3.

Then, substituting the unknown coefficients ν_{g1}, ν_{g2}, β_1 and β_2 in the Table 3 into the equations $MDL_{1,2} = |\beta_1 - \beta_2|L$ and $DMGD_{1,2} = |1/\nu_{g1} - 1/\nu_{g2}|$, the $MDL_{1,2}$ and $DMGD_{1,2}$ between LP_{01} and LP_{11a} modes are obtained, which are 0.186 dB and 3.581 ps/m, respectively.

TABLE 4
The Values of Unknown Coefficients ν_{g1}, ν_{g3}, β_1 and β_3

LP modes	ν_g [km/s]	β [dB/km]
LP_{01}	206781	0.232
LP_{11b}	206627	0.248

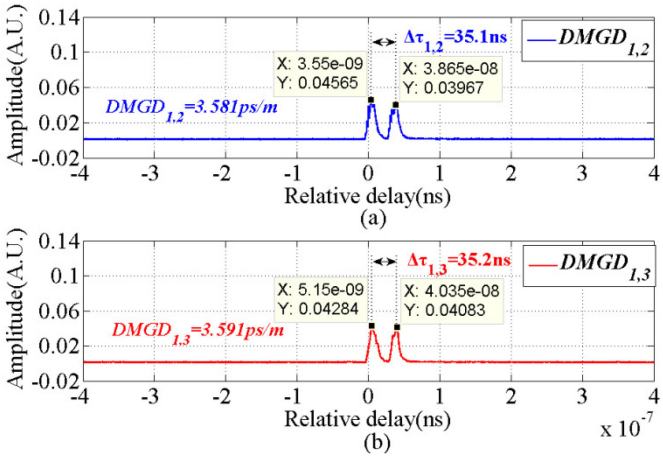

Fig. 6. Comparison of results measured with present method and TOF method. (a) $DMGD_{1,2}$ between the LP_{01} and LP_{11a} modes. (b) $DMGD_{1,3}$ between the LP_{01} and LP_{11b} modes.

We also carry out the measurement of $MDL_{1,3}$ and $DMGD_{1,3}$. Fig. 5(a) and 5(b) show the backscattered amplitudes of LP_{01} and LP_{11b} mode channels in the FUT when a 300 ns input optical pulse is coupled into the LP_{01} or LP_{11b} modes, respectively. Similarly, the four unknown coefficients ν_{g1}, ν_{g3}, β_1 and β_3 can be calculated as listed in Table 4. Thus, the $MDL_{1,3}$ and $DMGD_{1,3}$ can be simultaneously calculated by the equations $MDL_{1,3} = |\beta_1 - \beta_3|z$ and $DMGD_{1,3} = |1/\nu_{g1} - 1/\nu_{g3}|$ as 0.157 dB and 3.604 ps/m. These values agree well with the $MDL_{1,2}$ and $DMGD_{1,2}$ values of 0.186 dB and 3.581 ps/m between the LP_{01} mode and LP_{11a} modes, respectively. We know that, due to the strong mixing, no loss or delay difference should be observed for degenerate modes (LP_{11a} and LP_{11b} modes). However, the results of MDL and $DMGD$ measured between LP_{01} and LP_{11a} were slightly different from those measured between LP_{01} and LP_{11b}. The main reason is that the IL of LP_{11a} and LP_{11b} port of the PLs is different, and the crosstalk of the photonic lantern from LP_{01} mode to LP_{11a} and LP_{11b} modes is also different. Even though we have compensated for IL and crosstalk caused by photonic lanterns, etc. But due to the existence of IL and crosstalk measurement errors, the results measured between degenerate modes and LP_{01} mode are still slightly different.

Next, the conventional transmission measurement and TOF measurement [10] are implemented respectively in order to verify the effectiveness of our proposed method. First of all, we measured the impulse responses of fundamental mode and higher-order modes to calculate the DMGD. Fig. 6(a) and (b) show the measurement results of $DMGD_{1,2}$ and $DMGD_{1,3}$ with the TOF method, respectively. It can be concluded that the results measured by our proposed technique agree well with those obtain with the TOF method.

Then, we compare present results of MDL with those obtained with a conventional transmission method. To perform the transmission method, the insertion losses of the mode-converter (PL A) /demultiplexer (PL B) is measured previously. Since the LP_{11a} and LP_{11b} modes are degenerate modes, the coupling between them are strong in the case of slight pressure on the FMF. So, the value of the transmission loss is calculated by averaging the values of LP_{11a} and LP_{11b} modes.

TABLE 5
Comparison of MDL Measured With Our Proposed Method and Conventional Transmission Method

$MDL_{i,j}$	Present method	Transmission method	Difference between two methods
$MDL_{1,2}$	0.186dB	0.174 dB	0.012 dB
$MDL_{1,3}$	0.157 dB	(Average value)	-0.017 dB

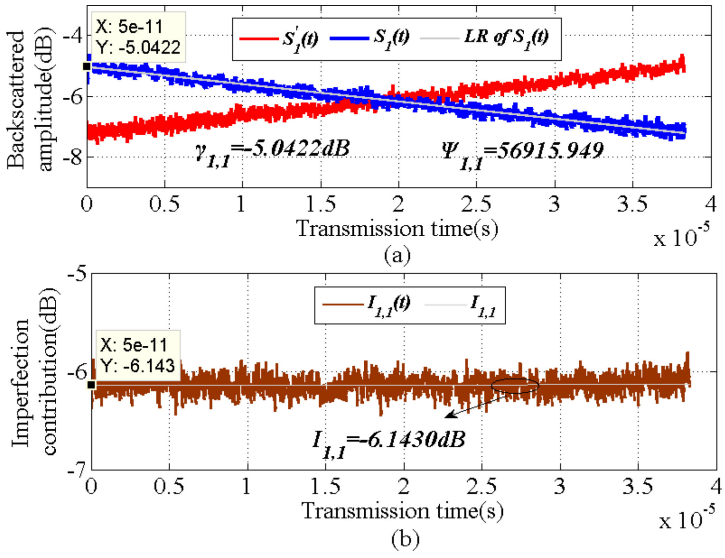

Fig. 7. The imperfection contribution $I_{1,1}$ for the LP_{01} mode. (a) Backscattered amplitudes for the LP_{01} mode measured from both ends of the FUT. (b) Imperfection contributions for the LP_{01} modes obtained from the results of Fig. 7(a).

Table 5 shows the measurement results of MDL obtain with the conventional transmission method. It is concluded that the measurement results of $MDL_{1,2}$ and $MDL_{1,3}$ measured using our proposed technique are in good agreement with those obtained with the conventional transmission method, respectively.

The experimental results presented above demonstrate that the proposed technique exhibits a similar level of measurement accuracy as its counterpart conventional transmission and TOF methods for measurement of MDL and DMGD, respectively. Moreover, compared with above two methods, the proposed method has the ability to simultaneously measure MDL and DMGD in FMFs.

4. Extension to Fibers With More Than Three Modes

In this section, we extend the proposed method to the measurement of 6-mode FMF as an example to demonstrate the ability for measuring fibers with large number of modes. The data processing is the same as described in Section 2. We take a step-index 6-mode FMF as FUT with the length of 4-km, which supports LP_{01}, $LP_{11a,b}$, $LP_{21a,b}$ and LP_{02} modes. Fig. 7(a) shows the backscattered amplitudes measured from both ends of the 6-mode fiber. The blue and red lines represent the amplitude for the LP_{01} mode of the backscattered light measured from both ends of FUT when a 300 ns input optical pulse is coupled into the LP_{01} mode at both ends of FUT, respectively. Fig. 7(b) shows imperfection contributions for the LP_{01} mode obtained from the results of Fig. 7(a). Figs. 8, 9 and 10 show the backscattered amplitudes for simultaneously measuring MDL and DMGD of FMFs between fundamental mode LP_{01} and every higher-order mode, respectively. The Rayleigh

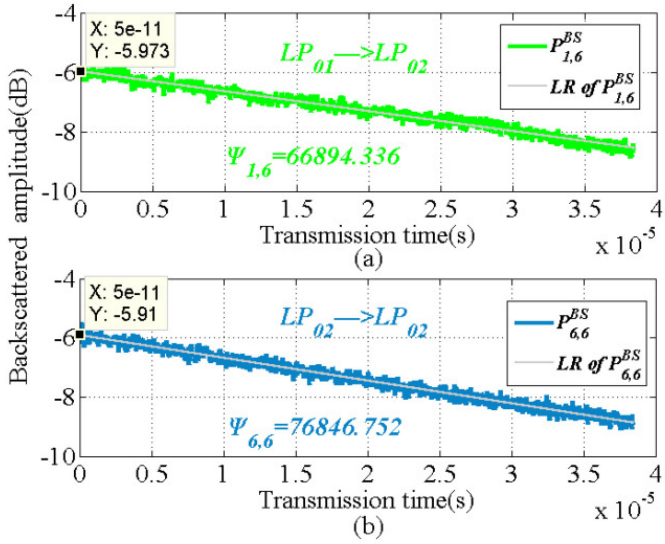

Fig. 8. Measurement results of $MDL_{1,6}$ and $DMGD_{1,6}$ between LP_{01} and LP_{02} modes. (a) Backscattered amplitude from the LP_{02} mode channel when a 300 ns optical pulse is coupled into the LP_{01} mode. (b) Backscattered amplitude from the LP_{02} mode channel when a 300 ns optical pulse is coupled into the LP_{11b} mode.

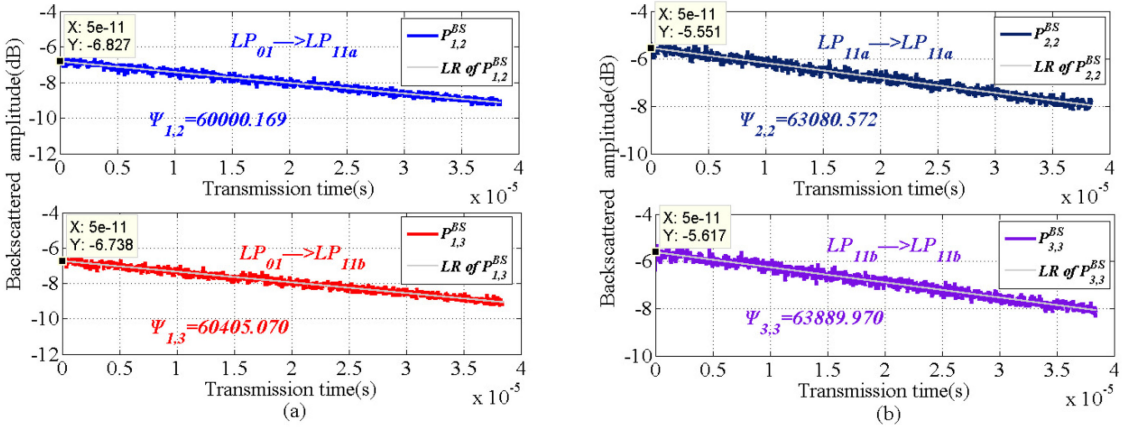

Fig. 9. Measurement results of $MDL_{1,2}$ and $DMGD_{1,2}$ between LP_{01} and LP_{11a} modes and $MDL_{1,3}$ and $DMGD_{1,3}$ between LP_{01} and LP_{11b} modes. (a) Backscattered amplitudes from the LP_{11a} and LP_{11b} mode channels when a 300 ns optical pulse is coupled into the LP_{01} mode. (b) Backscattered amplitudes from the LP_{11a} and LP_{11b} mode channels when a 300 ns optical pulse is coupled into the LP_{11a} and LP_{11b} modes, respectively.

backscattering amplitudes from the LP_{01}, $LP_{11a,b}$, $LP_{21a,b}$ and LP_{02} mode channels are obtained as shown in Figs. 8, 9 and 10 when the LP_{01} or $LP_{11a,b}$ or $LP_{21a,b}$ or LP_{02} mode is excited, respectively. Then, the parameters $I_{i,i}$, $\gamma_{i,i}$, $\psi_{i,i}$, $\psi_{j,j}$ and $\psi_{i,j}$ in Eqs. (6), (7) and (10) are obtained.

Substituting the acquired parameters [Figs. 7, 8, 9 and 10] into the Eqs. (6), (7) and (10), the unknown coefficients ν_{gi} and β_i can be acquired as listed in Table 6. Then, substituting the unknown coefficients into the equations $MDL_{1,j} = |\beta_1 - \beta_j|z$ and $DMGD_{1,j} = |1/\nu_{g1} - 1/\nu_{gj}|$, the $MDL_{1,j}$ and $DMGD_{1,j} (j = 2, 3, 4, 5, 6)$ can be obtained as 0.120 dB, 0.136 dB, 0.292 dB, 0.288 dB, 0.388 dB and 5.97 ps/m, 5.85 ps/m, 11.67 ps/m, 11.95 ps/m, 12.63 ps/m. The results are shown in Table 6. It can be seen from the measurement results that there are also slight difference in the MDL and DMGD

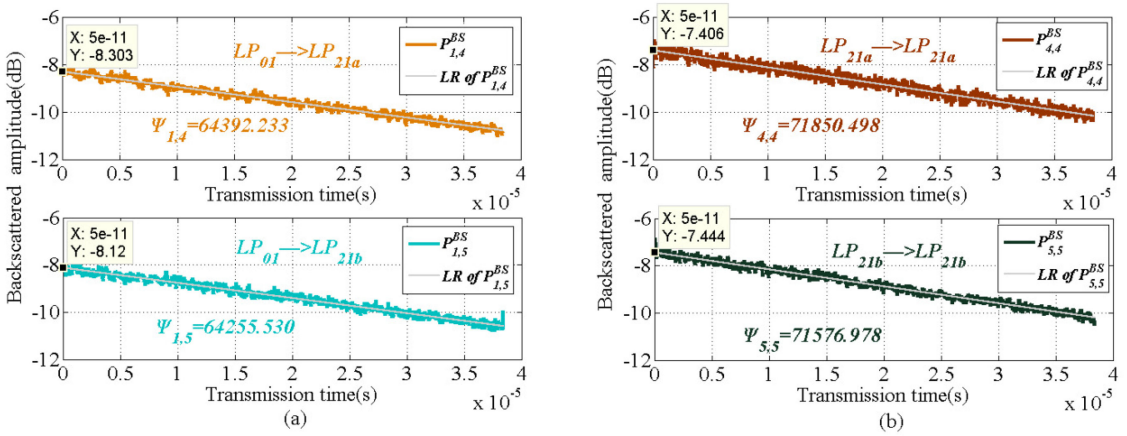

Fig. 10. Measurement results of $MDL_{1,4}$ and $DMGD_{1,4}$ between LP_{01} and LP_{21a} modes and $MDL_{1,5}$ and $DMGD_{1,5}$ between LP_{01} and LP_{21b} modes. (a) Backscattered amplitudes from the LP_{21a} and LP_{21b} mode channels when a 300 ns optical pulse is coupled into the LP_{01} mode. (b) Backscattered amplitudes from the LP_{21a} and LP_{21b} mode channels when a 300 ns optical pulse is coupled into the LP_{21a} and LP_{21b} modes, respectively.

TABLE 6
Summary of the Measurement Results of the 6-Mode Fiber

LP modes	v_g [km/s]	DMGD [ps/m]	β [dB/km]	MDL [dB]
LP_{01}	206817	0	0.275	0
LP_{11a}	206562	5.97	0.305	0.120
LP_{11b}	206567	5.85	0.309	0.136
LP_{21a}	206319	11.67	0.348	0.292
LP_{21b}	206307	11.95	0.347	0.288
LP_{02}	206278	12.63	0.372	0.388

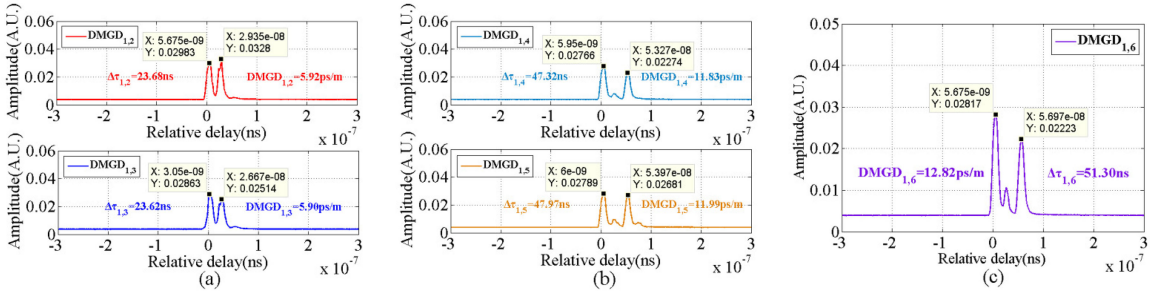

Fig. 11. Comparison of DMGD measured with our proposed method and TOF method. (a) $DMGD_{1,2}$ between the LP_{01} and LP_{11a} modes and $DMGD_{1,3}$ between LP_{01} and LP_{11b} modes. (b) $DMGD_{1,4}$ between the LP_{01} and LP_{21a} modes and $DMGD_{1,5}$ between LP_{01} and LP_{21b} modes. (c) $DMGD_{1,6}$ between the LP_{01} and LP_{02} modes.

between LP_{01} mode and degenerate modes. Moreover, the impairment value increases with the raise of mode order.

The proposed method is also compared with TOF method to testify the veracity of the $DMGD_{1,j}$ measurement results. The $DMGD_{1,j}$ between LP_{01} and LP_{11a}, LP_{11b}, LP_{21a}, LP_{21b} and LP_{02} values obtained with TOF method are given in Fig. 11. Due to mode coupling from excited mode to unexcited mode in FMF, small spikes appear in the amplitude distributions along relative delay as

TABLE 7
Comparison of MDL Measured With our Proposed Method and Conventional Transmission Method

$MDL_{i,j}$	Present method	Transmission method	Difference between two methods
$MDL_{1,2}$	0.120 dB	0.158 dB	-0.038 dB
$MDL_{1,3}$	0.136 dB	(Average value)	-0.022 dB
$MDL_{1,4}$	0.292 dB	0.289dB	0.003 dB
$MDL_{1,5}$	0.288 dB	(Average value)	-0.001 dB
$MDL_{1,6}$	0.388 dB	0.394 dB	-0.006 dB

shown in Fig. 11(b) and 11(c) when a 10 ns optical pulse is coupled into LP_{01} and $LP_{21a,b}$ [Fig. 11(b)] and LP_{01} and LP_{02} modes [Fig. 11(c)]. As can be seen, the results of TOF agree well with those obtained by proposed method.

The conventional transmission method in measuring $MDL_{1,j}$ of 6-mode fiber is conducted to compare with the proposed method. The $MDL_{1,j}$ values obtained with the conventional transmission method are summarized in Table 7. It's found that the results of these two methods are almost corresponding to each other.

5. Conclusion

We proposed and experimentally demonstrated a simple technique for measuring MDL and DMGD of FMFs simultaneously. We performed the measurements on 3-mode FMFs by analyzing the Rayleigh backscattering amplitudes obtained using a nondestructive measurement system, yielding results consistent with those obtained by the conventional transmission and TOF methods, respectively, and the principle and experiment presented here apply to FMFs supporting more than three modes based on the experiment on a 6-mode fiber. Moreover, the theory and experiment presented here apply to FMFs supporting more than 3 LP modes based on the experiment on a 6-LP-mode fiber. Thus we believe that our proposed technique is helpful to evaluate the quality and characterize the parameters of FMFs whether in the fiber manufacture or in the cabling case. Besides, it will benefit in the performance improvement of large-capacity MDM systems.

References

[1] G. Li, N. Bai, N. Zhao, and C. Xia, "Space-division multiplexing: The next frontier in optical communication," *Adv. Opt. Photon.*, vol. 6, no. 4, pp. 413–487, Dec. 23, 2014.
[2] G. Rademacher *et al.*, "Long-haul transmission over few-mode fibers with space division multiplexing," *J. Lightw. Technol.*, vol. 36, no. 6, pp. 1382–1388, Mar. 15. 2018.
[3] D. J. Richardson, J. M. Fini, and L. E. Nelson, "Space-division multiplexing in optical fibres," *Nature Photon.*, vol. 7, no. 5, pp. 354–362, Apr. 29. 2013.
[4] J. Du, D. Xie, C. Yang, and J. Wang, "Demonstration of analog links using spatial modes in km-scale few mode fiber," *Opt. Exp.*, vol. 25, no. 4, pp. 3613–3620, Feb. 20. 2017.
[5] D. Lee *et al.*, "A sparsity managed adaptive MIMO equalization for few-mode fiber transmission with various differential mode delays," *J. Lightw. Technol.*, vol. 34, no. 8, pp. 1754–1761, Apr. 15. 2016.
[6] L. Grünernielsen *et al.*, "Few mode transmission fiber with low DGD, low mode coupling, and low loss," *J. Lightw. Technol.*, vol. 30, no. 23, pp. 3693–3698, Dec. 1. 2012.
[7] K. Shibahara *et al.*, "Signal processing techniques for DMD and MDL mitigation in dense SDM transmissions," in *Proc. Opt. Fiber Commun. Conf. Exhib.*, Mar. 2017, Paper M2D.3.
[8] T. Mori, T. Sakamoto, M. Wada, T. Yamamoto, F. Yamamoto, and K. Nakajima, "Experimental verification of signal quality difference induced by differential modal loss and modal crosstalk on optical MIMO transmission and its compensation by equipartition multiplexing," *J. Lightw. Technol.*, vol. 34, no. 3, pp. 918–927, Feb. 1. 2016.
[9] R. Gabet *et al.*, "Complete dispersion characterization of few mode fibers by OLCI technique," *J. Lightw. Technol.*, vol. 33, no. 6, pp. 1155–1160, Mar. 15. 2015.
[10] J. Cheng *et al.*, "Time-domain multimode dispersion measurement in a higher-order-mode fiber," *Opt. Lett.*, vol. 37, no. 3, pp. 347–349, Feb. 1. 2012.

[11] T. Ahn, Y. Jung, K. Oh, and D. Kim, "Optical frequency-domain chromatic dispersion measurement method for higher-order modes in an optical fiber," *Opt. Exp.*, vol. 13, no. 25, pp. 10040–10048, Dec. 2. 2005.
[12] Z. Yang, N. Zhao, L. Zhang, R. Mi, and G. Li, "Simultaneous measurement of chromatic and modal dispersion in FMFs using microwave photonic techniques," *IEEE Photon. J.*, vol. 9, no. 3, Jun. 2017, Art. no. 5501409.
[13] N. K. Fontaine, "Characterization of space-division multiplexing fibers using swept-wavelength interferometry," in *Proc. Opt. Fiber Commun. Conf. Exhib.*, Mar. 2015, Paper W4I.7.
[14] J. Li *et al.*, "Modal dispersion characterization of few-mode fiber based on electrical spectral interferometry with optical frequency comb," *Opt. Fiber. Technol.*, vol. 38, pp. 75–79, Aug. 25. 2017.
[15] S. Ohno *et al.*, "Distributed spatial mode dispersion measurement along strongly coupled multicore fibers based on the correlation analysis of Rayleigh backscattering amplitudes," *Opt. Exp.*, vol. 25, no. 24, pp. 29650–29658, Nov. 13. 2017.
[16] H. Kubota *et al.*, "Mode-dependent loss measurement of a two-mode fiber using a conventional OTDR," *IEICE Commun. Exp.*, vol. 11, no. 11, pp. 429–434, Sep. 9. 2016.
[17] M. Nakazawa, M. Yoshida, and T. Hirooka, "Measurement of mode coupling distribution along a few-mode fiber using a synchronous multi-channel OTDR," *Opt. Exp.*, vol. 22, no. 25, pp. 31299–31309, Dec. 11. 2014.
[18] M. Nakazawa, M. Yoshida, and T. Hirooka, "Nondestructive measurement of mode couplings along a multi-core fiber using a synchronous multi-channel OTDR," *Opt. Exp.*, vol. 20, no. 11, pp. 12530–12540, May. 18. 2012.
[19] M. Ohashi, H. Kubota, Y. Miyoshi, and R. Maruyama, "Longitudinal fiber parameter measurements of two-mode fiber links by using OTDR," in *Proc. Eur. Conf. Opt. Commun.*, Sep. 2014, Paper Th.1.4.5.
[20] A. Nakamura, K. Okamoto, Y. Koshikiya, and T. Manabe, "Effective mode field diameter for LP_{11} mode and its measurement technique," *IEEE Photonic. Technol. Lett.*, vol. 28, no. 22, pp. 2553–2556, Nov. 15. 2016.
[21] M. Ohashi *et al.*, "Longitudinal fiber parameter measurements of multi-core fiber using OTDR," *Opt. Exp.*, vol. 22, no. 24, pp. 30137–30147, Nov. 25. 2014.
[22] Z. Wang, H. Wu, X. Hu, N. Zhao, Q. Mo, and G. Li, "Rayleigh scattering in few-mode optical fibers," *Sci. Rep.*, vol. 6, Oct. 24. 2016, Art. no. 35844.
[23] A. Nakamura *et al.*, "High-sensitivity detection of fiber bends: 1-μm-band mode-detection OTDR," *J. Lightw. Technol.*, vol. 33, no. 24, pp. 4862–4869, Dec. 1. 2015.